Placenta to cartilage: direct conversion of human placenta to chondrocytes with transformation by defined factors

Ryuga Ishii[a,b,*], Daisuke Kami[a,c,*], Masashi Toyoda[a,c], Hatsune Makino[a], Satoshi Gojo[c], Toshiharu Ishii[b], and Akihiro Umezawa[a]

[a]Department of Reproductive Biology and Pathology, National Research Institute for Child Health and Development, Tokyo 157-8535, Japan; [b]Department of Pathology, Toho University School of Medicine, Tokyo 143-8540, Japan; [c]Tokyo Metropolitan Geriatric Hospital and Institute of Gerontology, Tokyo 173-0015, Japan

ABSTRACT Cellular differentiation and lineage commitment are considered to be robust and irreversible processes during development. Recent work has shown that mouse and human fibroblasts can be reprogrammed to a pluripotent state with a combination of four transcription factors. We hypothesized that combinatorial expression of chondrocyte-specific transcription factors could directly convert human placental cells into chondrocytes. Starting from a pool of candidate genes, we identified a combination of only five genes (5F pool)—*BCL6*, *T* (also called *BRACHYURY*), *c-MYC*, *MITF*, and *BAF60C* (also called *SMARCD3*)—that rapidly and efficiently convert postnatal human chorion and decidual cells into chondrocytes. The cells generated expressed multiple cartilage-specific genes, such as *Collagen type II α1*, *LINK PROTEIN-1*, and *AGGRECAN*, and exhibited characteristics of cartilage both in vivo and in vitro. Expression of the endogenous genes for *T* and *MITF* was initiated, implying that the cell conversion is due to not only the forced expression of the transgenes, but also to cellular reprogramming by the transgenes. This direct conversion system from noncartilage tissue to cartilaginous tissue is a substantial advance toward understanding cartilage development, cell-based therapy, and oncogenesis of chondrocytes.

INTRODUCTION

The possibility of redirecting cell differentiation by overexpression of genes was suggested by H. Weintraub with the identification of the "master gene," *MyoD* (Davis *et al.*, 1987). The process was believed to involve reversion to a less differentiated state, a kind of dedifferentiation, before the new cell type is formed. Another process has since been introduced—the concept of direct conversion or direct reprogramming without dedifferentiation. This process is believed to be direct lineage switching rather than lineage switching back to a branch point and out again in a different direction (Hochedlinger and Jaenisch, 2006; Orkin and Zon, 2008). Direct conversion has been shown in β cells, cardiomyocytes, and neurons. A specific combination of three transcription factors (*Ngn3*, *Pdx1*, and *MafA*) reprograms differentiates pancreatic exocrine cells in adult mice into cells that closely resemble β cells (Zhou *et al.*, 2008); a combination of three factors (*Gata4*, *Tbx5*, and *Baf60c*) induces noncardiac mesoderm to differentiate directly into contractile cardiomyocytes (Ieda *et al.*, 2010); and a combination of three factors (*Ascl1*, *Brn2*, and *Myt1l*) converts mouse fibroblasts into functional neurons (Vierbuchen *et al.*, 2010). In this study, we used the strategy of direct conversion to generate chondrocytes from human somatic cells.

During skeletal development, chondrogenesis starts from condensed mesenchyme tissue, which differentiates into chondrocytes and begins secreting the molecules that form the extracellular matrix and leads to endochondral ossification. Cartilage is a stiff yet flexible connective tissue found in many areas in the bodies of humans and other animals. It is composed of chondrocytes, which

FIGURE 1: Characterization of infected cells. (A) Cell source for infection. Smooth chorion- and decidua-derived cells were used to investigate chondrogenesis by direct reprogramming. Bars, 1 mm. (B) Cell cultivation. (a) Phase contrast micrograph of parental cells. Bars indicate 200 μm. (b) Growth curve of parental cells. (C) Cells infected with five genes. (a) Phase contrast micrograph of infected cells. Bars, 200 μm. (b) Growth curve of infected cells. Orange, clone 01; red, clone 02; blue, clone 03; green, clone 05. Vertical axis indicates population doublings (PDs), and horizontal axis indicates days after infection. (D) Quantitative RT-PCR of *TERT* expression in the infected cell lines (clones 01, 02, 03, and 05). Individual RNA expression levels were normalized to respective *GAPDH* expression levels. HeLa cells were used for reference. Error bars, SD (n = 3). (E) Genomic DNA PCR analysis of uninfected and infected cells. To investigate chromosomal integration of the genes by retroviral infection, we performed genomic DNA PCR analysis, using transgene-specific primers of each gene. Five transgenes (*BCL6, T, c-MYC, MITF,* and *BAF60C*) were detected in all of the infected cell lines. (F) Southern blot analyses of the infected cells (clone 01). Genomic DNA was digested with *Spe*I, *Mfe*I, *Bgl*II, *Nco*I, and *Bam*HI and then probed for probes of the genes for *BCL6, T, c-MYC, MITF,* and *BAF60C*, respectively. The transgenes (*BCL6, T, c-MYC, MITF,* and *BAF60C*) were detected in all of the infected cell lines. Arrows indicate bands corresponding to the endogenous genes. (G) STR analysis of

produce a large amount of collagen fiber, an abundant ground substance rich in proteoglycans, and elastin fibers. Developmentally, the undifferentiated mesenchymal cells migrate into the limb field and condense to form the cartilage anlage. Bone morphogenic proteins and transforming growth factor-β initiate the chondrogenic program and have significant effects on chondrogenesis through distinct mechanisms in a stage-specific manner. In addition to soluble factors, the high mobility group–domain transcription factors such as *Sox5, Sox6,* and *Sox9* control chondrogenic differentiation, maintain the chondrocyte phenotype, and regulate expression of extracellular matrix molecules, such as cartilage-specific collagen type II (Lefebvre *et al.*, 1997).

Murine chondrocytes can be converted from fetal fibroblasts by the direct reprogramming method using the cartilage-specific transcription factors *Sox9, c-Myc,* and *Klf4* (Hiramatsu *et al.*, 2011), but human chondrocytes converted from different types of cells have not yet been reported. In the present study, we generated chondrosarcoma cell lines derived from human placenta by the direct reprogramming method, using a different set of genes. Placental membrane can be obtained at every delivery and is usually discarded. Therefore it is an easily accessible cellular source without ethical problems.

RESULTS

Isolation of cells from smooth chorion and decidua

We used smooth chorion and decidua for a cell source by removing the amnion from the placental membrane and used the explant culture method in which the cells are outgrown from pieces of smooth chorion and decidua attached to dishes (Figure 1A and Supplemental Figure S1). The adherent chorion- and decidua-derived cells were passaged when the cells reached ~80% confluence. These placenta-derived cells continued to grow for 30 d, which was five population doublings (PDs), before reaching senescence (Figure 1B). The cells at four PDs were used as "parental cells" for conversion analysis.

parental cells and the infected cells. All of the infected cells exhibited the same STR patterns as parental cells. (H) G-band chromosome analysis for parental cells with XX chromosomes and infected cells 01. (I) G-band chromosome analysis for parental cells with XY chromosomes and infected cells 05.

Infection of transcription factors into placenta-derived cells

To select candidates for transcription factors that would be required to reprogram fibroblasts to a cartilage fate, we used microarray analyses to identify transcription factors and chromatin remodeling factors with greater expression in mouse embryonic stem cell that are differentiated into mesoderm. We started with a 14-gene set, that is, genes for mesoderm-specific transcription factors (*T*, *MITF*, *TBX5*, *TBX20*, *CSX/NKX2.5*, *GATA4*, *MEF2C*, *MESP1*, *ISL1*, *BCL6*, and *PRDM16*) and chromatin-remodeling/reprogramming factors (*BAF60C*, *c-MYC*, and *KLF4*). We generated individual retroviruses to efficiently express each gene. Viral infections were preceded by transfection of small interfering RNA (siRNA) to the *p53* gene (Supplemental Figure S2). Parallel experiments using retrovirus carrying the EGFP gene indicated that infection efficiency was nearly 100%. We investigated expression of cartilage-associated genes such as *Collagen Type II α1* (*COL2A1*), *Collagen Type X α1* (*COL10A1*), *LINK PROTEIN-1* (*CRTL1*), and *AGGRECAN* (*ACAN*) by reverse transcriptase (RT)-PCR and identified five genes (*BCL6*, *T*, *c-MYC*, *MITF*, and *BAF60C*) that induced chondrocyte gene expression. The induction levels of the cartilage-associated genes were greatly reduced by elimination of any one gene from the five-gene set. We thus decided to use the five-gene set for chondrogenic induction for subsequent experiments. After we seeded infected cells on mouse embryonic fibroblasts (MEFs), we detected a very large number of mouse embryonic stem cell–like colonies on MEFs 15 d after infection of the 5F pool (Figure 1C, a). Efficiency of colony formation (colony number per the number of cells infected) was 5.76 ($\pm$0.21) $\times$ 10^{-4}. We randomly picked four clones and analyzed cell growth rates. The cells replicated at a rate of once every 2 d and continued to grow for >150 d without reaching senescence (Figure 1C, b). All four clones expressed the *TERT* gene after establishment as a cell line (Figure 1D). The cells infected with the five genes exhibited a chondrogenic phenotype with malignant transformation, as shown by following results, and were thus designated induced chondrosarcoma (iCS) cells.

To determine chromosomal insertion of the genes, we performed genomic DNA PCR analysis (Figure 1E). The genes encoding BCL6, T, c-MYC, MITF, and BAF60C were detected in chromosomal genome of the four clones. Southern blot analysis with cDNA probes of each of the five genes (*BCL6*, *T*, *c-MYC*, *MITF*, and *BAF60C*) confirmed that each clone had chromosomal integration of the exogenously infected genes (Figure 1F and Supplemental Figure S3). The analysis of the 16 short tandem repeats (STRs) revealed that the infected clones were derived from parental cells: clones 1, 2 and 3 were derived from parental cells of the same donor with XX chromosomes, and clone 5 was derived from different parental cells with XY chromosome (Figure 1G). The STR patterns of the infected cells differed from those of any cell lines deposited on National Institutes of Health website (http://stemcells.nih.gov/research/nihresearch/scunit/genotyping .htm), implying that the cells generated are not a contamination of previously established cell lines. To determine the karyotypes of the iCS cell lines, karyotypic analysis was performed at different passages (P6– P23). Chromosomal G-band analyses showed that each clone had a normal karyotype with 46XX and 46XY (Figure 1, H and I, respectively). We then performed karyotypic analysis on iCS clones after prolonged passages (P15 and P23 for iCS-01; P13 and P21 for iCS-02; P12 and P21 for iCS-03; P7 and P23 for iCS-05, and did not detect any significant karyotypic change (Supplemental Figure S4).
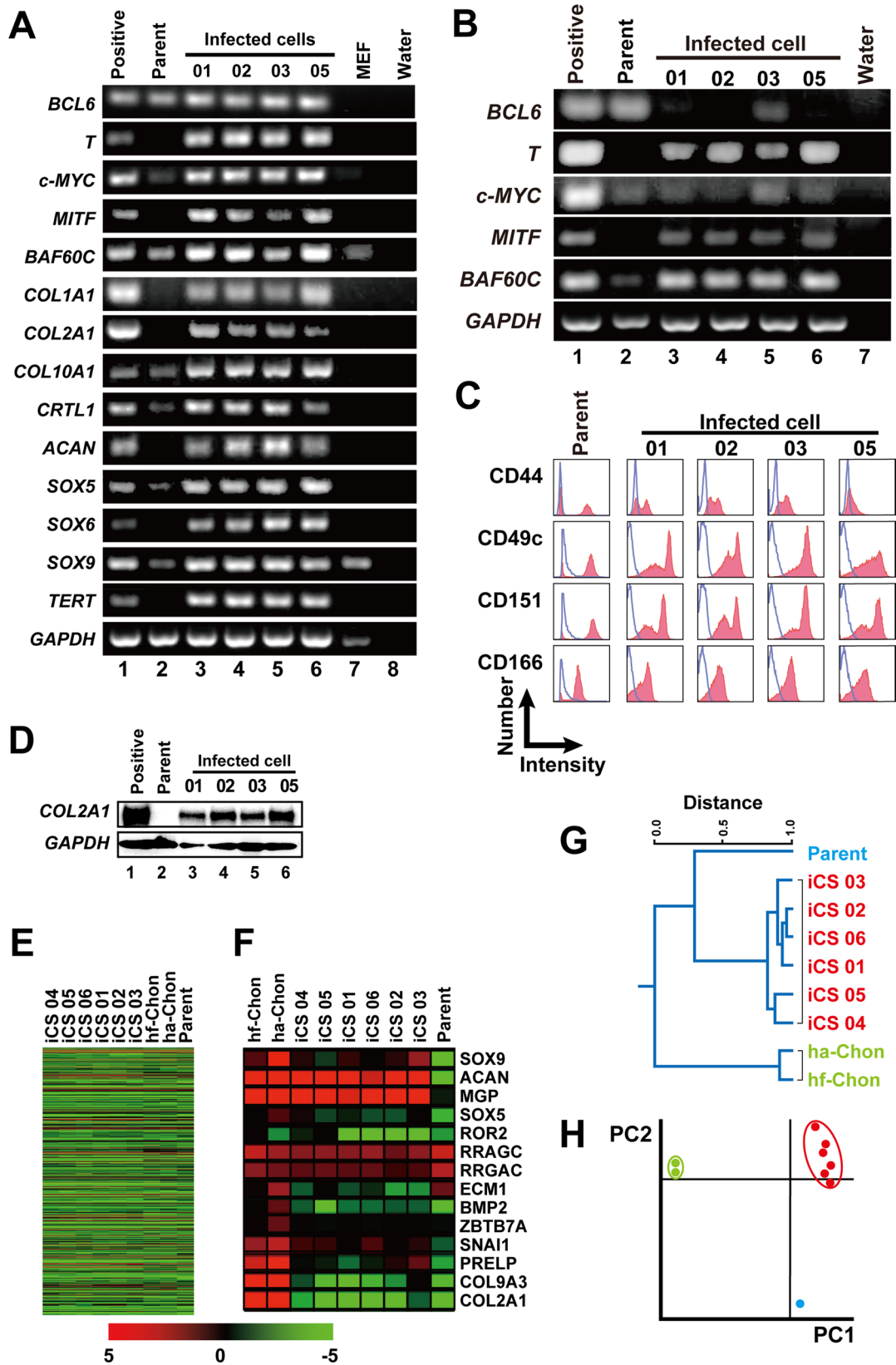
In vitro chondrogenic phenotypes of the cells infected with the 5F pool

To investigate whether the infected cells exhibit a chondrogenic phenotype in vitro, we performed RT-PCR analysis using primers of the cartilage-specific genes (Figure 2A and Supplemental Table S1; Sekiya *et al.*, 2002; Shirasawa *et al.*, 2006). All the cell lines expressed the chondrocyte-specific/associated transcription factors (*SOX5*, *SOX6*, and *SOX9*), structural genes (*COL1A1*, *COL2A1*, *CRTL1*, and *ACAN*), and immortalizing gene (*TERT*). To see whether the endogenous genes for *BCL6*, *T*, *c-MYC*, *MITF*, and *BAF60C* were expressed by reprogramming, we performed RT-PCR analysis by the primers specific to the endogenous gene but not the transgenes (Supplemental Figure S5). Endogenous genes such as *T*, *MITF*, and *BAF60C* were induced (Figure 2B). To determine the surface markers of the cells, we performed flow cytometric analysis. All clones were positive for CD44, CD49c, CD151, and CD166 but not CD117 and CD133, suggesting that the cell marker pattern of iCS cells is compatible with that of chondrocytes (Figure 2C; Grogan *et al.*, 2007). Western blot analysis revealed that all the infected cells expressed COL2A1 and COL1A1 at the protein level (Figure 2D and Supplemental Figure S6). Comprehensive gene expression analysis showed that the expression pattern of the infected cells is similar to that of human adult chondrocytes and human fetal chondrocytes (Figure 2E). Expression of cartilage-specific genes such as *Sox9*, *Aggrecan*, and *Matrix Gla-protein* was detected in the infected cells and chondrocytes but not in the parent human smooth chorion and decidua cells (Figure 2F). Conversely, expression of placenta-associated genes such as *GATA3*, *CD200*, *PDCD1LG2*, *OLR1*, *TEK*, *HSD17B2*, and *FOXF1* was lost in the infected cells. Hierarchical clustering analysis revealed that the infected cells were grouped into the same category that includes chondrocytes obtained from human fetuses and adults (Figure 2G). In addition, principal component analysis (PCA) revealed that the infected cells and chondrocytes showed similar scores in the PC2 axis (Figure 2H). The representative genes (principal components) of the PC2 axis in Table 1 include cartilage-specific genes such as *Aggrecan*, *Fibromodulin*, and *Matrix Gla-protein* (Plaas and Wong-Palms, 1993; Yagami *et al.*, 1999; Sekiya *et al.*, 2002; Hjorten *et al.*, 2007; Surmann-Schmitt *et al.*, 2009).

Inhibition of five factors by small interfering RNA

To investigate the involvement of the five factors in chondrogenesis, we suppressed their expression by siRNA (Supplemental Table S2). The mRNAs for the five factors (*BCL6*, *T*, *c-MYC*, *MITF*, and *BAF60C*) were significantly decreased by siRNAs compared with control cells transfected with control siRNAs (Figure 3, A and B, and Supplemental Figures S7–S9). Morphological changes in the siRNA-treated cells were too variable to interpret. Gene expression of the chondrogenic-specific/associated transcription factors (*SOX5*, *SOX6*, and *SOX9*) and structural genes (*COL1A1*, *COL2A1*, *CRTL1*, and *ACAN*) decreased significantly in si*T* (siRNA to the *T* gene)-transfected cells compared with cells treated with control siRNA (Figure 3C and Supplemental Figure S10), suggesting that *T* is necessary for chondrogenic conversion (Hoffmann *et al.*, 2002). In addition, expression of the genes for *SOX5*, *SOX6*, *COL1A1*, and *COL2A1* decreased significantly in si*MITF*-transfected cells compared with cells transfected with control siRNA, suggesting that *MITF* is also necessary for chondrogenic conversion. In contrast, treatment of siRNA to *BCL6*, *c-MYC*, and *BAF60C*) did not alter cartilage-related genes (Zelzer and Olsen, 2003; Levy and Fisher, 2011). si*MITF* diminished the cobblestone appearance of iCS colonies and the cell lining at the periphery of iCS colonies and altered the appearance of the iCS cells to a fibroblast-like morphology, which may be related to decreased expression of the cartilage-associated genes.

FIGURE 2: Chondrogenic phenotypes of infected cells. (A) RT-PCR analysis of the genes encoding cartilage-specific proteins (SOX5, SOX6, SOX9, COL1A1, COL2A1, COL10A1, CRTL1, and ACAN), immortalizing gene (TERT), and the infected genes (BCL6, T, c-MYC, MITF, and BAF60C). Primers that detect both the transgenes and endogenous genes for BCL6, T, c-MYC, MITF, and BAF60C were used (Supplemental Figure S5C). RNAs from the following sources were used for positive controls: heart for BCL6, MITF, BAF60C, and GAPDH; iPS cells for T, c-MYC, and TERT; and cartilage for COL1A1, COL2A1, COL10A1, CRTL1, ACAN, SOX5, SOX6, and SOX9. H$_2$O (water without RNA) served as a

Gene symbol	Description	Gene symbol	Description
ACAN	Aggrecan	CLEC4D	C-type lectin domain family 4, member D
FMOD	Fibromodulin	NRAP	Nebulin-related anchoring protein
MGP	Matrix Gla protein	OR2V2	Olfactory receptor, family 2, subfamily V, member 2
LRRC48	Leucine-rich repeat containing 48		
SLPI	Secretory leukocyte peptidase inhibitor	KCNH7	Potassium voltage-gated channel, subfamily H (eag-related), member 7
RAB11FIP4	RAB11 family interacting protein 4 (class II)	KCNK17	Potassium channel, subfamily K, member 17
TLR5	Toll-like receptor 5		
NEBL	Nebulette	DRD1	Dopamine receptor D1
RAB11FIP4	RAB11 family interacting protein 4 (class II)	CTNNA2	Catenin (cadherin-associated protein), α2
CAPG	Capping protein (actin filament), gelsolin-like	FMR1NB	Fragile X mental retardation 1 neighbor
SLC26A4	Solute carrier family 26, member 4	ABCC12	ATP-binding cassette, subfamily C (CFTR/MRP), member 12
MIF	Macrophage migration inhibitory factor (glycosylation-inhibiting factor)		
		SLITRK3	SLIT and NTRK-like family, member 3
CALR3	Calreticulin 3	CIITA	Class II, major histocompatibility complex, transactivator
ESPN	Espin		
SLC7A2	Solute carrier family 7 (cationic amino acid transporter, y+ system), member 2	GP2	Glycoprotein 2 (zymogen granule membrane)
CHRNA4	Cholinergic receptor, nicotinic, α4	OR12D3	Olfactory receptor, family 12, subfamily D, member 3
ZBTB10	Zinc finger and BTB–domain containing 10		
ND3	NADH-ubiquinone oxidoreductase chain 3(NADH dehydrogenase subunit 3)	GALNTL4	UDP-N-acetyl-α-D-galactosamine
		BRSK2	BR serine/threonine kinase 2
EFNA1	Ephrin-A1	L08961	Transmembrane tyrosine kinase mRNA
RGMA	RGM domain family, member A	RAB33B	RAB33B, member RAS oncogene family
ENST00000390243	Immunoglobulin κ light-chain V gene segment	ELA1	Elastase 1, pancreatic
		ASPA	Aspartoacylase (Canavan disease)
GPA33	Glycoprotein A33 (transmembrane)	IL18RAP	Interleukin 18 receptor accessory protein
CLMN	Calmin (calponin-like, transmembrane)	EPHA8	EPH receptor A8
RAB11FIP4	RAB11 family interacting protein 4 (class II)	CXCR6	Chemokine (C-X-C motif) receptor 6
KRT26	Keratin 26	BAGE	B melanoma antigen
YBX2	Y box–binding protein 2	SIRPG	Signal-regulatory protein γ
EEF1G	Eukaryotic translation elongation factor 1 γ	AF083118	CATX-2 mRNA
NAG18	NAG18 protein on chromosome 19	TSPAN16	Tetraspanin 16
CX62	Connexin 62	AF028840	Kruppel-associated box protein mRNA
KCNC2	Potassium voltage-gated channel, Shaw-related subfamily, member 2	WIF1	WNT inhibitory factor 1
		TTTY9A	Testis-specific transcript, Y-linked 9A (TTTY9A) on chromosome Y
TSPAN33	Tetraspanin 33		
PTCH1	Patched homologue 1 (*Drosophila*)	LRRC50	Leucine-rich repeat containing 50
DEFB126	Defensin, β126	ENST0000037416	Collagen, type XXVII, α1
RAMP3	Receptor (G protein–coupled) activity–modifying protein 3	WFDC12	WAP four-disulfide c ore domain 12

TABLE 1: Representative genes in PC2 axis of the PCA.

negative control. (B) RT-PCR analysis of the endogenous genes encoding T, MITF, and BAF60C. The primers were prepared to amplify the endogenous genes but not the transgenes. RNAs from the following sources were used for positive controls: heart for BCL6, MITF, BAF60C, and GAPDH; and iPS cells for T and c-MYC. H_2O (water without RNA) served as a negative control. (C) Flow cytometric analysis of cell surface markers on the parental cells and infected cells. All of the results were compared with each isotype control. The *X*- and *Y*-axes indicate the intensity and the cell number, respectively. (D) Western blot analysis of COL2A1 protein in the infected cells and parental cells. (E, F) The heat map in the infected cells and parental cells. Each row represents a gene; each column represents a cell population. Expression levels of representative genes are shown in F. (G) Hierarchical clustering analysis (TIGR MeV; see *Materials and Methods*), based on expression levels of the cartilage-associated genes. (H) Principal component analysis of gene expression levels.
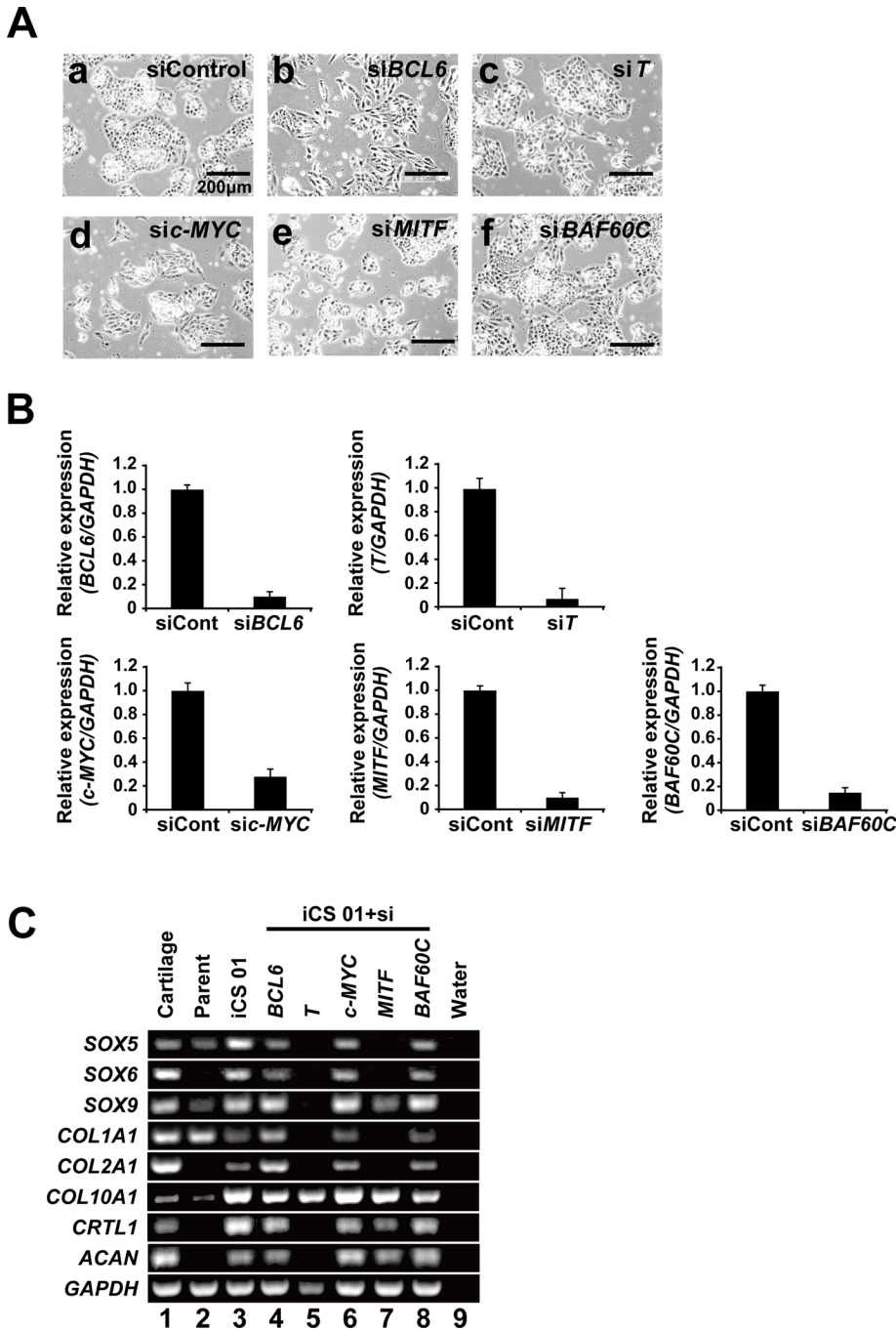
FIGURE 3: Functional effect of genes in iCS cells. (A) Phase contrast microscopic views.
(a) Control siRNA–treated iCS cells. (b) *BCL6* siRNA–treated iCS cells. (c) *T* siRNA–treated iCS cells.
(d) *c-MYC* siRNA–treated iCS cells. (e) *MITF* siRNA–treated iCS cells. (f) *BAF60C* siRNA–treated
iCS cells. Bars, 200 μm. (B) Quantitative RT-PCR of each gene in siRNA-treated cells. Individual
RNA expression levels were normalized to respective *GAPDH* expression levels. Error bars,
mean ± SD (*n* = 3). (C) RT-PCR analysis of the genes encoding SOX5, SOX6, SOX9, COL1A1,
COL2A1, COL10A1, CRTL1, and ACAN. Human cartilage and H$_2$O (water without RNA) served
as positive and negative controls, respectively.

## Cartilage formation after implantation of the cells infected with the 5F pool

To investigate whether iCS cells exhibit a chondrogenic pheno-
type in vivo, we intradermally injected the cells into dorsal flanks
of immunodeficient Balb/c nu/nu mice. The masses generated
underwent histopathological analysis 7 wk after injection. The

injected cells generated cartilage that ex-
hibited metachromasia by toluidine blue
staining and were light blue when stained
with Alcian blue (Figure 4A). In contrast,
implantation of parental cells produced
neither tumor nor cartilage (Figure 4E).
RT-PCR analysis showed that iCS cartilage
expressed genes for *COL1A1*, *COL2A1*,
COL10A1, *CRTL1*, *ACAN*, CD44, CD49c,
CD151, and CD166 (Figure 4B). Western
blot analysis showed that iCS cartilage pro-
duced collagen type II at the protein level
(Figure 4C). We also performed immuno-
histochemical analysis using antibodies to
vimentin, collagen type II, and Ki-67. The
antibody for vimentin that we used specifi-
cally reacts with human protein but not mu-
rine protein. The antibody for Ki-67 reacts
with a human nuclear cell proliferation–as-
sociated antigen, and thus it does not react
with differentiated chondrocytes. iCS cells
stained positive for human vimentin, and
extracellular matrix was positive for colla-
gen type II, implying that the injected hu-
man cells generate cartilage (Figure 4D).
Nearly 30% of iCS cells stained positive for
Ki-67, indicating that iCS cells continued to
replicate in cartilage at 7 wk after injection.
iCS cells in the tumor had large nuclei with
coarse chromatin structure and one or two
nucleoli, and the ratio of nucleus/cyto-
plasm was large. The tumors generated by
iCS cells were histopathologically diag-
nosed as chondrosarcoma by a certified
pathologist (A.U.). Anchorage-indepen-
dent colony formation is a hallmark of
transformation and an in vitro correlate of
tumorigenicity in vivo (Cremona and Lloyd,
2009). After cultivation in MethoCult H4034
medium, colony formation was evaluated
(Figure 5). The colony-forming assay clearly
revealed that iCS cells formed colonies but
parental cells did not, indicating that iCS
cells are transformed cells with chondro-
genic potential.

Generation of chondrocytes from other human somatic cells

In addition to human smooth chorion, we
used primary cultured cells from human
menstrual blood and placental artery. We
obtained 10 and 9 clones, respectively,
from menstrual blood–derived cells and
placental arterial endothelium. All of them
proliferated as a chondrogenic cells with
transformation and exhibited the same
morphology with iCS in vitro (Figure 6). The growth rates of the
clones generated from menstrual blood and placental artery
were essentially the same as those of iCS cells. After implanta-
tion into the dermal tissue of nude mice, they generated chon-
drogenic tissue that showed metachromasia with the toluidine
blue stain.
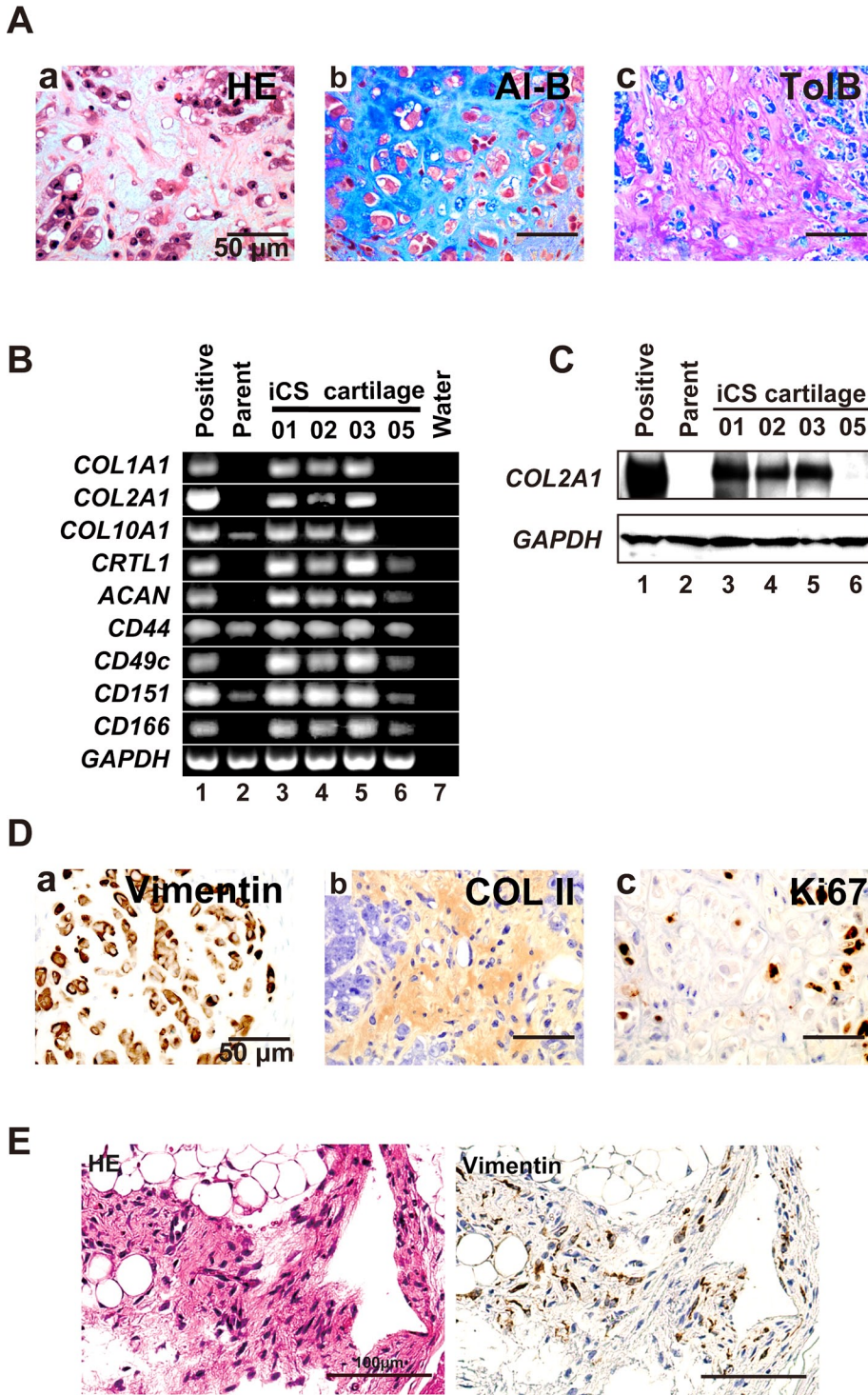
FIGURE 4: In vivo chondrogenic phenotypes of iCS cells. (A) Cartilage at 7 wk after injection of iCS cells. (a) HE stain, (b) Alcian blue, (c) toluidine blue. iCS cells at passage 3 were injected subcutaneously to the dorsal flank of athymic nude mice. Areas of extracellular matrix accumulation stain light to dark blue with Alcian blue (b) or light- to dark-red/purple with toluidine blue (c). Bars, 50 μm. These results are representative of five independent experiments. (B) RT-PCR analysis of the genes encoding SOX5, SOX6, SOX9, COL1A1, COL2A1, COL10A1, CRTL1, and ACAN in cartilage generated by iCS cells. Human cartilage and H$_2$O (water without RNA) served as positive and negative controls, respectively. Parental cells in culture serve for comparison. (C) Western blot analysis of COL2A1 protein in iCS cartilage at 7 wk after subcutaneous injection of iCS cells into athymic nude mice. Human cartilage serves a positive control. GAPDH was used as a loading control. (D) Immunohistochemical analysis of iCS cartilage. (a) Vimentin, (b) collagen type II (COL II), (c) Ki-67. (E) Implantation of the parental cells. We injected parental cells into athymic nude mice but did not detect any tumor formation.

DISCUSSION

In mammals, cartilage does not regenerate in limb tissue, but cells that derive cartilage retain a strong memory of their embryonic origin in the axolotl (Kragl et al., 2009). Cells are undergoing reprogramming that allows them to reenter embryonic programs of tissue formation, even if they do not revert back to the pluripotent state. Here we show that expression of five transcription factors can rapidly and efficiently convert nonchondrocytes (chorion- and decidua-derived cells) into chondrocytes. iCS cells displayed functional chondrogenic properties such as the generation of extracellular matrices. The possibility of redirecting cell differentiation by overexpression of genes was suggested by Weintraub with the identification of the *MyoD* "master" gene (Davis et al., 1987). The process was believed to involve reversion to a less differentiated state, a kind of dedifferentiation, before the new cell type is formed. Another process has since been suggested, the concept of direct conversion or direct reprogramming without dedifferentiation. This process is believed to be direct lineage switching rather than lineage switching back to a branch point and out again in a different direction. Direct conversion has been shown in β cells, cardiomyocytes, and neurons. A specific combination of three transcription factors (*Ngn3*, *Pdx1*, and *MafA*) reprograms differentiated pancreatic exocrine cells in adult mice into cells that closely resemble β cells (Zhou et al., 2008); a combination of three factors (*Gata4*, *Tbx5*, and *Baf60c*) induces noncardiac mesoderm to differentiate directly into contractile cardiomyocytes (Ieda et al., 2010); and a combination of three factors (*Ascl1*, *Brn2*, and *Myt1l*) converts mouse fibroblasts into functional neurons (Vierbuchen et al., 2010). In this study, we used the strategy of direct conversion to generate chondrocytes from human extraembryonic somatic cells. Based on the same method, murine chondrocytes were generated from skin fibroblasts (Hiramatsu et al., 2011) using the three transcription factors *Sox9*, *c-Myc*, and *Klf4*. *Sox9* is a determinant of chondrogenic lineage (Lefebvre et al., 1997), *c-Myc* is a cell cycle driver (Schmidt, 1999), and *Klf4* is involved in the down-regulation of *p53* (Rowland

We performed histological analysis and immunohistochemical analysis using the human vimentin-specific antibody. The parental cells did not exhibit cartilage formation at the injected site. Left, HE stain. Right, immunohistochemistry using human-specific antibody to vimentin. Bars, 100 μm.

A

Parent | iCS 01 | iCS 02 | iCS 03 | iCS 05
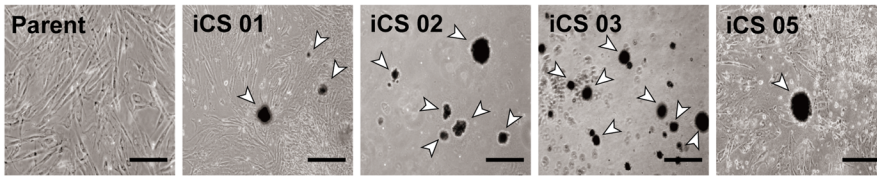
B
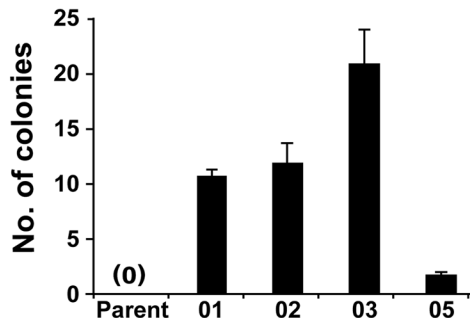
FIGURE 5: Colony formation of iCS cells. (A) Phase contrast micrograph of iCS colonies. iCS cells were cultured in methylcellulose medium on six-well plate dishes. Bars, 500 μm. (B) Number of iCS colonies. Error bars, SD ($n = 9$).

et al., 2005). In this study, *T* and *MITF* may act as inducers of chondrogenic fate determinant, and *BAF60C* may act as epigenetic modifier. *Klf4* was unnecessary for conversion from placental cells to chondrocytes, unlike the reprogramming described for iPS cells (Takahashi and Yamanaka, 2006) and chondrocytes (Hiramatsu *et al.*, 2011). *Baf60c* permits binding of *Gata4* to cardiac genes for reprogramming toward cardiomyocytes (Takeuchi and Bruneau, 2009). Likewise, *BAF60C* may initiate expression of chondrogenic gene sets in combination with *T* and *MITF* in iCS cells.

We showed that the transgene set was sufficient for chondrogenesis without exogenous *SOX9* gene. The *T* gene, one of the transcription factors used in this study, is a member of the T-box family of transcription factors (Papaioannou and Silver, 1998), all of which play key roles during early development, mostly in the formation and differentiation of normal mesoderm (Showell *et al.*, 2004). *T* is also transiently induced in vitro in rhesus monkey embryonic stem cells and mouse embryonal carcinoma cells undergoing mesodermal differentiation (Vidricaire *et al.*, 1994; Behr *et al.*, 2005). Both *T* and *Sox9* are downstream of mitogen-activated protein kinase signaling via fibroblast growth factor receptors in chondrogenesis (Hoffmann *et al.*, 2002). Chondrogenic conversion of the human extraembryonic cells was accompanied by induction of the endogenous *Sox9* gene; however, the induced *Sox9* did not complement reduction of chondrogenesis by siRNA to the *T* gene. *MITF* was also shown to be involved in chondrogenic conversion, although involvement of *MITF* in chondrogenesis has not been reported. *MITF* belongs to an evolutionarily ancient family of the bHLH/LZ proteins (Atchley and Fitch, 1997) and is known to regulate a number of genes of importance in differentiation and maintenance of the melanocytic lineage (Tachibana *et al.*, 1996); conversely, loss-of-function mutations in *MITF* produce depigmentation (Newton *et al.*, 2001). Disruption of *MITF* does not affect chondrocytic differentiation during development, and alternative factors may therefore be present in cells of chondrogenic lineage. The chondrogenesis by *T* and *MITF* may not reflect developmental or physiological pathway, but these

two factors are requisite for in vitro chondrogenic conversion of nonchondrocytes.

Stability of the chondrogenic phenotype of iCS cells after long-term cultivation is probably due to lack of transgene silencing—in other words, continuity of transgene expression during cultivation and expression of endogenous chondrogenic genes in some cases. Chondrogenic induction is mediated at least in part by reprogramming, because expression of the endogenous *T* gene was initiated by the five factors. It remains unclear whether the process of the conversion is via dedifferentiation into multipotent, oligopotent stem cells or undifferentiated progenitors. Placenta is developmentally distinct from cartilage, and conversion from placenta to chondrocytes is considered lineage switching or transdifferentiation rather than differentiation. In β cells (Zhou *et al.*, 2008) and retinal cells (Osakada *et al.*, 2009), direct reprogramming is achieved with hepatocytes and iris cells, respectively, which are developmentally close to the generated cells. Successful reprogramming with other somatic cells for parental cells (Figure 6) indicates that the conversion is indeed reprogramming. Autoregulatory feedback and feedforward activation of downstream transcriptional regulators reinforces the expression of important cell fate–determining genes and helps to further stabilize the induced transcriptional program. Robust changes in transcriptional activity can be explained by genome-wide adjustments of repressive and active epigenetic features, such as DNA methylation, histone modifications, and changes of chromatin-remodeling complexes that further stabilize the new transcriptional network (Zhou *et al.*, 2008). It is possible that certain subpopulations of cells are "primed" to respond to these factors, depending on their preexisting transcriptional or epigenetic states (Yamanaka, 2009).

Our study opens an avenue to generate human chondrocytes. Even with the presence of retroviral integration, human iCS cells can possibly be used for tissue engineering experiments such as screening of suitable scaffold of cartilage and can be an alternative to murine ATDC5 teratocarcinoma cells, an ideal cell line for development of tissue engineering strategies aimed at cartilage generation. Once the safety issue, that is, cell transformation, is overcome, iCS cells should also be applicable for repair of defective cartilage in regenerative medicine. We should, however, exercise caution because human iCS cells are not identical to human chondrocytes from the viewpoint of global gene expression. Further studies are essential to determine whether a nontransformed counterpart of iCS can replace chondrocytes in medical applications.

MATERIALS AND METHODS
Preparation of tissue and procedure for cell culture
A human placenta was collected after delivery of a male neonate with the approval of the Ethics Committee of the National Research Institute for Child Health and Development, Tokyo, Japan. Signed informed consent was obtained from the donors, and the specimens were irreversibly deidentified. All experiments handling human cells and tissues were performed in line with the Tenets of the Declaration of Helsinki. This study was wholly carried out at the National Research Institute for Child Health and Development, Tokyo, Japan.

A
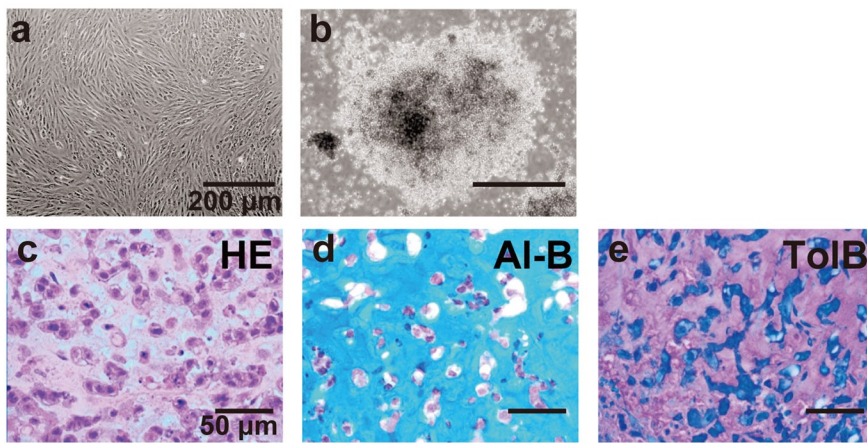
B
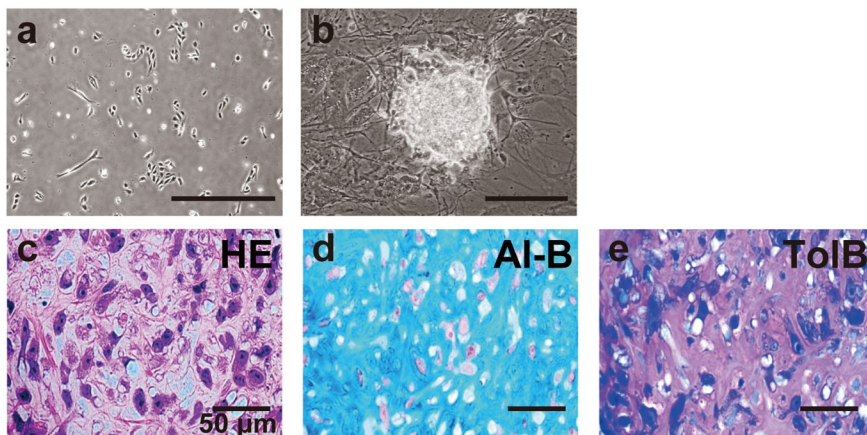
FIGURE 6: Generation of iCS cells from other human somatic cells. (A) iCS generation from human menstrual blood. (a) Phase contrast micrograph of menstrual blood–derived cells. (b) Phase contrast micrograph of iCS cells from menstrual blood. (c–e) Histological analysis of iCS cartilage generated from menstrual blood. (c) HE stain, (d) Alcian blue (AI-B), (e) toluidine blue (TolB). Bars, 200 (a, b) and 50 μm (c–e). (B) iCS generation from human placental artery (hPAE). (a) Phase contrast micrograph of hPAE cells. (b) Phase contrast micrograph of iCS cells from hPAE cells. (c–e) Histological analysis of iCS cartilage generated from hPAE cells. (c) HE stain, (d) Alcian Blue (Al-B), (e) toluidine blue (TolB). Bars, 200 μm (a, b) and 50 μm (c–e).

To isolate placenta-derived cells, we used the explant culture method, in which the cells were outgrown from pieces of chorion and decidual cells attached to dishes (Supplemental Figure S1). Briefly, the smooth chorion and decidua were cut into pieces ~2 mm^3 in size. The pieces were washed in DMEM (high glucose; Sigma-Aldrich, St. Louis, MO) supplemented with 100 U/ml penicillin–streptomycin (Life Technologies, Carlsbad, CA), 1 μg/ml amphotericin B (Life Technologies), and 4 U/ml Novo-Heparin Injection 1000 (Mochida Seiyaku, Tokyo, Japan) until the supernatant was free of erythrocytes. Some pieces were attached to the substratum in a 10-cm dish. The cells migrated out from the cut ends after ~20 d of incubation at 37°C in 5% CO$_2$. The migrated cells were harvested with Dulbecco's phosphate-buff-

ered saline with 0.1% trypsin and 0.25 mM EDTA for 5 min at 37°C and counted. The harvested cells were reseeded at a density of 3×10^5 cells in a 10-cm dish. Confluent monolayers of cells were subcultured at a 1:8 split ratio onto new 10-cm dishes. The culture medium was replaced with fresh culture medium every 3 or 4 d.

Plasmid construction

Full-length of transcription factors *BCL6*, *T*, *c-MYC*, *MITF*, and *BAF60C* were amplified from cDNAs prepared from total RNA of adult human heart cells (Clontech, Mountain View, CA) and embryonic body-formed iPS cells (day 3–4) by reverse transcription-PCR with the primers listed in Supplementary Table 1, and by digestion with *Hind*III sites of pMXs and T4 DNA polymerase accessory they were used for DNA synthesis. The cDNA plasmid was subcloned into pMXs vector using *Hind*III restriction sites. pMXs was a gift from T. Kitamura (Tokyo University, Tokyo, Japan).

Retroviral infection

293FT cells (5×10^6) were plated in a 10-cm dish and incubated overnight. The next day, the cells were cotransfected with pMXs-*BCL6*, pMXs-*T*, pMXs-*c-MYC*, pMXs-*MITF*, pMXs- *BAF60C*, pCL-GagPol, and pHCMV-VSV-G vectors with TransIT-293 reagent (Mirus, Madison, WI). The medium was replaced with fresh medium 24 h after transfection. The medium was collected after 48 h as the virus-containing supernatant. Placenta-derived cells in primary culture were seeded at 1×10^5 cells per six-well plate 1 d before infection. The virus-containing supernatants were filtered through a 0.45-μm pore-size filter, ultracentrifuged at $8000 \times g$ for 24 h, and then resuspended in Knockout-DMEM (Invitrogen) supplemented with 2 mg/ml Polybrene (Nacalai Tesque, Kyoto, Japan). Cells in six-well plates were transfected with siRNA to the *p53* gene (si*TP53*) using RNAiMAX (Invitrogen, Carlsbad, CA) according to the protocols recommended by the manufacturer (Hong *et al.*, 2009). Cells were transfected overnight, washed, and resus-

pended in Opti-MEM (Life Technologies/Invitrogen) and were used for virus infection. Cells were trypsinized and plated in six-well plates at 1×10^5 cells per well for 24 h before transfection. Retrovirus cocktail was transferred to cells and incubated for 24 h. After infection, cells were cultured for 5 d and replaced on an irradiated MEF feeder layer in six-well plates. The medium was changed every 2 d with fresh Poweredby10 (GP Biosciences, Yokohama, Japan). Colonies were picked up and transferred into 2-ml Poweredby10 medium at ~10 d after infection. The colonies were mechanically dissociated to small clumps by pipetting up and down. The cell suspension was transferred on irradiated MEF feeder in 60-mm dish (Iwaki; Asahi Techno Glass, Tokyo, Japan). We defined this stage as passage 1.

RT-PCR

Total cellular RNA was isolated from cells using an Isogen extraction kit (Nippon Gene, Tokyo, Japan) according to the manufacturer's protocol. Total RNA (1.0 µg each) for RT-PCR was converted to cDNA with Superscript III RNase H– reverse transcriptase (Invitrogen), according to the manufacturer's manual. PCR conditions were optimized, and the linear amplification range was determined for each primer by varying annealing temperature and cycle number. PCR products were identified by positive control size. Primer sequences are provided in Supplemental Table S1 and Supplemental Figure S5. RT-PCR was performed by using the primers for the genes *BCL6*, *T*, *c-MYC*, *MITF*, *BAF60C*, *COL1A1*, *COL2A1*, *COL10A1*, *CRTL1*, *ACAN*, *SOX5*, *SOX6*, *SOX9*, *TERT*, and *GAPDH*. Adult chondrocyte RNA (Cell Applications (San Diego, CA), human heart RNA (Clontech), and human iPS cell RNA were used as positive controls for RT-PCR analysis. PCR was performed with KOD FX DNA polymerase and PCR buffer (Toyobo, Osaka, Japan), 35 cycles, with each cycle consisting of 95°C for 30 s, 60°C for 45 s, and 72°C for 45 s, with additional 5-min incubation at 72°C after completion of the final cycle. The PCR products were size fractionated by 2% agarose gel electrophoresis.

Quantitative RT-PCR

RNA was extracted from cells using an Isogen extraction kit according to the manufacturer's protocol. An aliquot of total RNA was reverse transcribed by using an oligo(dT) primer. For the thermal cycle reaction, the cDNA template was amplified (PRISM 7900HT Sequence Detection System; Applied Biosystems, Foster City, CA) using the Platinum Quantitative PCR SuperMix-UDG with ROX (11743-100; Invitrogen) under the following reaction conditions: 40 cycles of PCR (95°C for 15 s, and 60°C for 1 min) after an initial denaturation (95°C for 2 min). Fluorescence was monitored during every PCR cycle at the annealing step. The authenticity and size of the PCR products were confirmed using a melting curve analysis (using software provided by Applied Biosystems) and gel analysis. mRNA levels were normalized using *GAPDH* as a housekeeping gene.

Flow cytometric analysis

Cells were stained for 1 h at 4°C with primary antibodies and immunofluorescent secondary antibodies. The cells were then analyzed on a Cytomics FC 500 (Beckman Coulter, Brea, CA), and the data were analyzed with FlowJo, version 7 (Tree Star, Ashland, OR). Antibodies against human CD44, CD49c, CD151, and CD166 (all from BD Biosciences PharMingen, San Diego, CA) were adopted as primary antibodies.

Histological analysis

Infected cells were harvested by trypsin/EDTA treatment, collected into tubes, and centrifuged at 300 × *g* for 5 min, and the pellets were suspended in the DMEM medium. The same volume of Basement Membrane Matrix (BD Biosciences PharMingen) was added to the cell suspension. The cells were implanted subcutaneously to a BALB/c-nu/nu mouse (CREA, Tokyo, Japan) for 7 wk. Tumors were dissected and fixed with phosphate-buffered saline containing 4% paraformaldehyde. Paraffin-embedded tissue was sliced and stained with hematoxylin and eosin.

Western blotting

Semiconfluent cells were lysed with CelLytic M cell Lysis Reagent (Sigma-Aldrich) supplemented with a protease inhibitor cocktail (Sigma-Aldrich). Cell lysates (20 µg each) were separated by electrophoresis on NuPAGE Novex Tris-Acetate gel (Invitrogen), and transferred to Immobilon-P transfer membrane (Millipore, Billerica, MA).

The membrane was soaked in protein blocking solution (Blocking One solution; Nacalai Tesque) for 30 min at room temperature before an overnight incubation at 4°C with primary antibody for COL2A1 (1:1000; Santa Cruz Biotechnology, Santa Cruz, CA) and GAPDH (1:1000; Cell Signaling, Beverly, MA) also diluted in blocking solution. The membrane was then washed three times with TBST (20 mM Tris-HCl, pH 7.6, 136 mM NaCl, and 0.1% Tween-20), incubated with a horseradish peroxidase–conjugated secondary antibody (0.04 µg/ml) directed against the primary antibody for 45 min, and washed three times with TBST. The signal was detected by an enhanced ECL Plus Western Blotting Detection System (GE Healthcare, Piscataway, NJ) and an LAS3000 imaging system (Fujifilm, Tokyo, Japan), following the manufacturers' recommendations.

siRNA transfection

The infected cells in six-well plates were transfected with siRNA using Lipofectamine RNAiMAX Reagent (Invitrogen) according to the protocols recommended by the manufacturer (Cui *et al.*, 2011). The cells were harvested 48 h after transfection and analyzed by real-time PCR and RT-PCR.

Gene expression microarray

Total RNA was prepared from duplicate biological samples, and human adult chondrocyte RNA was purchased from Cell Applications. With the use of Low RNA Input Fluorescent Linear Amplification Kits (Agilent Technologies, Santa Clara, CA), cDNA was reverse transcribed from each RNA sample, as well as from a pooled reference control, and cRNA was then transcribed and fluorescently labeled with Cy3. cRNA was purified using an Agilent One Color Spike Mix Kit (Agilent Technologies). We hybridized 1650 ng of Cy3-labeled and amplified cRNA to Agilent 4 × 44 K whole human genome microarrays and processed it according to the manufacturer's instructions. The array was scanned using a G2505B DNA microarray scanner (Agilent Technologies). The image files were extracted using Feature Extraction software, version 10.7.3.1 (Agilent Technologies), with background subtraction and dye normalization. The data were analyzed using GeneSpring GX 10.0 (Agilent Technologies).

Hierarchical clustering analysis and principal component analysis

To analyze the microarray data, we used agglomerative hierarchical clustering and PCA. The hierarchical clustering techniques classify data by similarity using NIA Array Analysis (http://lgsun.grc.nia.nih.gov/ANOVA), and their results are represented by dendrograms. PCA is a multivariate analysis technique that finds major patterns in data variability using TIGR MeV (www.tm4.org/mev.html; Toyoda *et al.*, 2011).

Southern blot analysis

For Southern blot analysis, genomic DNA was isolated using the DNeasy kit (Qiagen, Valencia, CA) according to the manufacturer's protocol, digested with *Spe*I and *Bam*HI for *BCL6*, *Spe*I and *Nco*I for *BAF60C*, *Spe*I and *Bgl*II for *MITF* and *T*, and *Spe*I and *Mfe*I or *Bam*HI and *Mfe*I for *c-MYC*, and separated via 0.8% agarose gel electrophoresis. Transfer was to Hybond-N membranes (GE Healthcare). The membrane was fixed under UV irradiation. The probe was hybridized to the blot and detected using CDP-Star detection reagent (GE Healthcare). Signals from the labeled DNA were quantified using a Hyper film ECL (GE Healthcare).

Short-tandem repeat analysis

Genomic DNA was isolated from cultured cell samples using DNeasy columns (Qiagen). This was used as template for STR analysis using

the PowerPlex 16 System (Promega, Madison, WI) and PRISM instrumentation (Applied Biosystems). Numbers shown denote base pair lengths of the 15 autosomal fragments. The analysis was carried out at Nihon Gene Research Laboratories (Sendai, Japan).

Karyotypic analysis
The cells were fixed with methanol:glacial acetic acid (2:5) three times and dropped onto glass slides (Nihon Gene Research Laboratories). Chromosome spreads were Giemsa banded and photographed. A minimum of 10 metaphase spreads were analyzed for each sample, and they were karyotyped using a chromosome imaging analyzer system (Applied Spectral Imaging, Carlsbad, CA).

Colony formation assay
A total of 50,000 cells were resuspended in MethoCult H4034 medium and plated into a six-well plate. Colonies were counted 14 d after plating.

Gene Expression Omnibus accession numbers
National Center for Biotechnology Information Gene Expression Omnibus gene expression microarray data were submitted under accession number GSE29745.

REFERENCES
Atchley WR, Fitch WM (1997). A natural classification of the basic helix-loop-helix class of transcription factors. Proc Natl Acad Sci USA 94, 5172–5176.

Behr R, Heneweer C, Viebahn C, Denker HW, Thie M (2005). Epithelial-mesenchymal transition in colonies of rhesus monkey embryonic stem cells: a model for processes involved in gastrulation. Stem Cells 23, 805–816.

Cremona CA, Lloyd AC (2009). Loss of anchorage in checkpoint-deficient cells increases genomic instability and promotes oncogenic transformation. J Cell Sci 122, 3272–3281.

Cui CH, Miyoshi S, Tsuji H, Makino H, Kanzaki S, Kami D, Terai M, Suzuki H, Umezawa A (2011). Dystrophin conferral using human endothelium expressing HLA-E in the non-immunosuppressive murine model of Duchenne muscular dystrophy. Hum Mol Genet 20, 235–244.

Davis RL, Weintraub H, Lassar AB (1987). Expression of a single transfected cDNA converts fibroblasts to myoblasts. Cell 51, 987–1000.

Grogan SP et al. (2007). Identification of markers to characterize and sort human articular chondrocytes with enhanced in vitro chondrogenic capacity. Arthritis Rheum 56, 586–595.

Hiramatsu K, Sasagawa S, Outani H, Nakagawa K, Yoshikawa H, Tsumaki N (2011). Generation of hyaline cartilaginous tissue from mouse adult dermal fibroblast culture by defined factors. J Clin Invest 121, 640–657.

Hjorten R et al. (2007). Type XXVII collagen at the transition of cartilage to bone during skeletogenesis. Bone 41, 535–542.

Hochedlinger K, Jaenisch R (2006). Nuclear reprogramming and pluripotency. Nature 441, 1061–1067.

Hoffmann A et al. (2002). The T-box transcription factor Brachyury mediates cartilage development in mesenchymal stem cell line C3H10T1/2. J Cell Sci 115, 769–781.

Hong H, Takahashi K, Ichisaka T, Aoi T, Kanagawa O, Nakagawa M, Okita K, Yamanaka S (2009). Suppression of induced pluripotent stem cell generation by the p53-p21 pathway. Nature 460, 1132–1135.

Ieda M, Fu JD, Delgado-Olguin P, Vedantham V, Hayashi Y, Bruneau BG, Srivastava D (2010). Direct reprogramming of fibroblasts into functional cardiomyocytes by defined factors. Cell 142, 375–386.

Kragl M, Knapp D, Nacu E, Khattak S, Maden M, Epperlein HH, Tanaka EM (2009). Cells keep a memory of their tissue origin during axolotl limb regeneration. Nature 460, 60–65.

Lefebvre V, Huang W, Harley VR, Goodfellow PN, de Crombrugghe B (1997). SOX9 is a potent activator of the chondrocyte-specific enhancer of the pro alpha1(II) collagen gene. Mol Cell Biol 17, 2336–2346.

Levy C, Fisher DE (2011). Dual roles of lineage restricted transcription factors: the case of MITF in melanocytes. Transcription 2, 19–22.

Newton JM, Cohen-Barak O, Hagiwara N, Gardner JM, Davisson MT, King RA, Brilliant MH (2001). Mutations in the human orthologue of the mouse underwhite gene (uw) underlie a new form of oculocutaneous albinism, OCA4. Am J Hum Genet 69, 981–988.

Orkin SH, Zon LI (2008). Hematopoiesis: an evolving paradigm for stem cell biology. Cell 132, 631–644.

Osakada F, Jin ZB, Hirami Y, Ikeda H, Danjyo T, Watanabe K, Sasai Y, Takahashi M (2009). In vitro differentiation of retinal cells from human pluripotent stem cells by small-molecule induction. J Cell Sci 122, 3169–3179.

Papaioannou VE, Silver LM (1998). The T-box gene family. Bioessays 20, 9–19.

Plaas AH, Wong-Palms S (1993). Biosynthetic mechanisms for the addition of polylactosamine to chondrocyte fibromodulin. J Biol Chem 268, 26634–26644.

Rowland BD, Bernards R, Peeper DS (2005). The KLF4 tumour suppressor is a transcriptional repressor of p53 that acts as a context-dependent oncogene. Nat Cell Biol 7, 1074–1082.

Schmidt EV (1999). The role of c-myc in cellular growth control. Oncogene 18, 2988–2996.

Sekiya I, Vuoristo JT, Larson BL, Prockop DJ (2002). In vitro cartilage formation by human adult stem cells from bone marrow stroma defines the sequence of cellular and molecular events during chondrogenesis. Proc Natl Acad Sci USA 99, 4397–4402.

Shirasawa S, Sekiya I, Sakaguchi Y, Yagishita K, Ichinose S, Muneta T (2006). In vitro chondrogenesis of human synovium-derived mesenchymal stem cells: optimal condition and comparison with bone marrow-derived cells. J Cell Biochem 97, 84–97.

Showell C, Binder O, Conlon FL (2004). T-box genes in early embryogenesis. Dev Dyn 229, 201–218.

Surmann-Schmitt C et al. (2009). Wif-1 is expressed at cartilage-mesenchyme interfaces and impedes Wnt3a-mediated inhibition of chondrogenesis. J Cell Sci 122, 3627–3637.

Tachibana M, Takeda K, Nobukuni Y, Urabe K, Long JE, Meyers KA, Aaronson SA, Miki T (1996). Ectopic expression of MITF, a gene for Waardenburg syndrome type 2, converts fibroblasts to cells with melanocyte characteristics. Nat Genet 14, 50–54.

Takahashi K, Yamanaka S (2006). Induction of pluripotent stem cells from mouse embryonic and adult fibroblast cultures by defined factors. Cell 126, 663–676.

Takeuchi JK, Bruneau BG (2009). Directed transdifferentiation of mouse mesoderm to heart tissue by defined factors. Nature 459, 708–711.

Toyoda M et al. (2011). Lectin microarray analysis of pluripotent and multipotent stem cells. Genes Cells 16, 1–11.

Vidricaire G, Jardine K, McBurney MW (1994). Expression of the Brachyury gene during mesoderm development in differentiating embryonal carcinoma cell cultures. Development 120, 115–122.

Vierbuchen T, Ostermeier A, Pang ZP, Kokubu Y, Sudhof TC, Wernig M (2010). Direct conversion of fibroblasts to functional neurons by defined factors. Nature 463, 1035–1041.

Yagami K, Suh JY, Enomoto-Iwamoto M, Koyama E, Abrams WR, Shapiro IM, Pacifici M, Iwamoto M (1999). Matrix GLA protein is a developmental regulator of chondrocyte mineralization and, when constitutively expressed, blocks endochondral and intramembranous ossification in the limb. J Cell Biol 147, 1097–1108.

Yamanaka S (2009). Elite and stochastic models for induced pluripotent stem cell generation. Nature 460, 49–52.

Zelzer E, Olsen BR (2003). The genetic basis for skeletal diseases. Nature 423, 343–348.

Zhou Q, Brown J, Kanarek A, Rajagopal J, Melton DA (2008). In vivo reprogramming of adult pancreatic exocrine cells to beta-cells. Nature 455, 627–632.